Trans. JSASS Aerospace Tech. Japan
Vol. 18, No. 5, pp. 209-215, 2020
DOI: 10.2322/tastj.18.209

Spectroscopic Measurements of Microwave-discharged CO_2 Plasma for Mars Entry Conditions

By Keiyu HANDA,[1)] Masato FUNATSU,[1)] and Kenji SHIBUSAWA[2)]

[1)] *Graduate School of Science and Technology, Gunma University, Kiryu, Japan*
[2)] *Department of Industrial Engineering, National Institute of Technology, Ibaraki College, Hitachinaka, Japan*

(Received July 3rd, 2019)

Recently, various unmanned and manned Mars exploration programs have been proposed. To send a space vehicle safely to the ground of Mars, the vehicle needs to be protected from the aerodynamic heating. The accurate prediction of the aerodynamic heating is important for the design of safe and light-weight thermal protection system. For the accurate prediction, it is necessary to simulate the plasma generated behind the shock wave and to clarify its internal state. To investigate the state of the plasma, spectroscopic measurement is useful. We performed the spectroscopic measurements of carbon dioxide (CO_2) plasma generated using microwave discharge under the pressure condition during Mars entry. To investigate the basic characteristics of microwave-discharged CO_2 plasma, the spectra of the radiation were obtained in the wavelength region of 200 to 800 nm. As a result, carbon monoxide (CO) fourth positive bands, CO third positive bands, CO Ångström bands, and atomic oxygen lines were observed. Electronic excitation temperature was also estimated by the Boltzmann plot method for the atomic oxygen lines.

Key Words: Radiation, CO_2 Plasma, Microwave Discharge, Spectroscopic Measurement, Mars Entry

Nomenclature

A	:	transition probability, s^{-1}
C	:	constant common to the spectra of the same temperature and atom
E	:	energy of level, cm^{-1}
g	:	multiplicity
I	:	relative intensity, a.u.
k	:	Boltzmann constant, cm^{-1}/K
P	:	microwave incident power, W
p	:	pressure, kPa
T	:	temperature, K
z	:	altitude, km
λ	:	wavelength, nm
Subscripts		
1	:	lower level
2	:	upper level
21	:	transition from the upper level to the lower level
ex	:	electronic excitation
s	:	behind shock wave

1. Introduction

Mars exploration programs such as Mars 2020 and ExoMars are in progress now, and the landers have been developed for launch in 2020. Human mission to Mars based on Lunar Orbital Platform-Gateway is also considered in the future.[1)] Mars entry missions cannot be avoided to send landers onto the ground. Landers enter the Martian atmosphere at the Mach number of 20 or higher,[2)] and strong shock wave is generated ahead of the entry vehicle. In this moment, gas changes into plasma behind the shock wave, and the entry vehicle receives remarkable aerodynamic heating. It consists mainly of convective and radiative heating. Most of studies on thermal effects during Mars entry focus on convective heating. However, recent analysis shows that radiative heating can be greater than convective one in the wake.[3)] Therefore, understanding the radiative characteristics, especially IR radiation, is significant for the accurate prediction of aerodynamic heating.[3)] For investigation of radiative heating effects, it is necessary to understand the internal state of the plasma generated during Mars entry. The radiation reflects the internal state of the plasma, therefore spectroscopic measurements of the radiation enable the internal state to be estimated. There are already some studies investigating characteristics of carbon dioxide (CO_2) plasma for Mars entry.[4), 5)] Arc-heated wind tunnels and shock tubes are generally used to simulate the plasma in those studies. Microwave discharge was used in this study to investigate basic radiative characteristics of carbon monoxide (CO) and oxygen (O) in CO_2 plasma. The microwave-discharged plasma has an advantage that it can be easily generated without impurities from the electrodes. It is known that CO has perturbation in the $B^1\Sigma$ and $b^3\Sigma$ states.[6)] The radiative characteristics caused by the perturbation is not clear well. In the future, we will investigate it and discuss radiation mechanism of the plasma generated during Mars entry.

The objective of this study is to investigate the basic characteristics of microwave-discharged CO_2 plasma. The CO_2 plasma was generated under the predicted pressure condition during Mars entry, and the radiation was measured spectroscopically in the wavelength region of 200 to 800 nm. The differences of the radiative characteristics with the microwave incident power were investigated, and electronic excitation temperatures of the plasmas were estimated by the Boltzmann plot method for atomic oxygen lines.

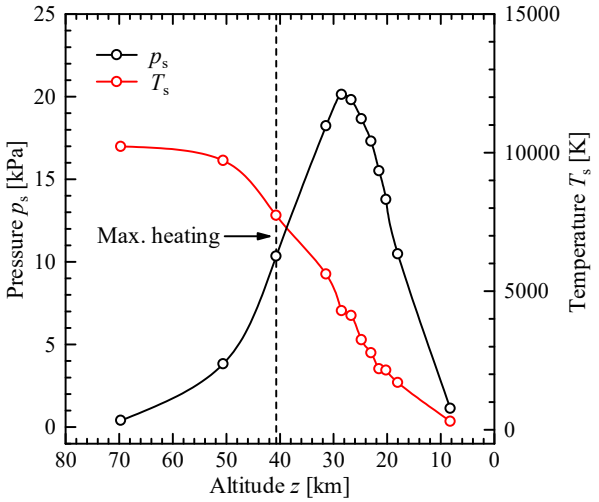

Fig. 1. Pressure and temperature behind shock wave.

2. Environments around Mars Entry Vehicle

Environments behind the shock wave depend on atmospheric conditions such as composition, pressure and temperature, and entry conditions such as shape of entry vehicle, velocity and entry angle. The Martian atmosphere consists of 96% CO_2, 1.9% Ar, 1.9% N_2 and 0.2% the others by volume, and CO_2 is the main component.[7] Martian atmospheric pressure and temperature are also different from ones of the Earth, thus environments behind the shock wave generated during Mars entry are different from ones during the Earth reentry. This section describes the estimations of pressure and temperature behind the shock wave under the entry conditions of Mars Pathfinder,[2] which is one of Mars entry vehicles. The pressure and temperature behind the shock wave are calculated preliminary using Rankine-Hugoniot equation,[8] assuming ideal gas, and the results are shown in Fig. 1. The horizontal axis means the altitude of Mars, the left axis means the pressure behind the shock wave p_s, and the right axis means the temperature behind the shock wave T_s. The state behind the shock wave proceeds from left to right in the figure when the entry vehicle descends. The pressure behind the shock wave increases to about 20 kPa at an altitude of 28 km and then decreases. The temperature behind the shock wave is about 10,000 K at an altitude of 70 km and decreases with the descent. Mars entry vehicle is predicted to receive a maximum of aerodynamic heating at an altitude of 41 km under the entry conditions of Mars Pathfinder.[2] The target pressure of experimental condition was determined as 1.3 kPa corresponding to the pressure behind the shock wave at an altitude of 63 km because of physical limitation of present experimental setup.

3. Experimental Setup and Methods

In this experiment, CO_2 plasma was generated under the pressure condition behind the shock wave and were measured spectroscopically. Figure 2 shows the schematic view of the experimental setup.[9] It is classified mainly into a microwave-discharged plasma generator and a section of spectroscopic measurement. In the microwave-discharged plasma

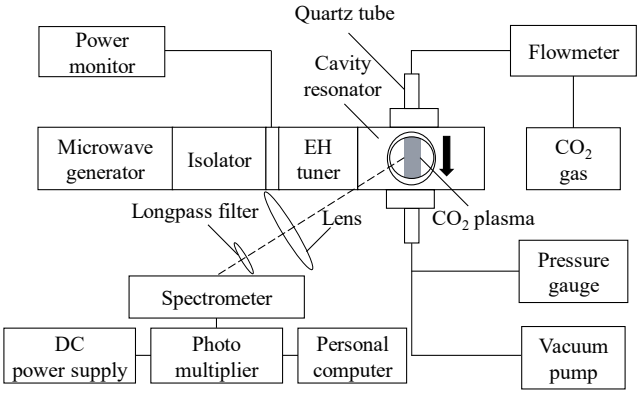

Fig. 2. Schematic view of experimental setup.

Table 1. Conditions of spectroscopic measurement.

Blaze wavelength	Longpass filter	Wavelength region
300 nm	-	200 - 400 nm
	320 nm	350 - 612 nm
500 nm	400 nm	400 - 800 nm

generator, a quartz tube with an inside diameter of 10 mm was inserted into the aperture of the resonator. Pure CO_2 gas was forced to flow in the tube and was exhausted by a vacuum pump. The microwave of the frequency of 2.45 GHz was generated by a microwave generator (TE-MG800C-IK, Tamaoki Electronics) and transmitted into the cavity resonator through an isolator (IM-1500, Micro Denshi) and an EH tuner (TM-5000/M, Micro Denshi). Some of the forward wave of microwave is absorbed to generate plasma, and the other is reflected. The forward wave power and the reflected wave power were measured using a power monitor (PM5000, Micro Denshi), and the difference between them is defined as the incident power. CO_2 plasma was generated in the tube while flowing CO_2 gas. The target pressure in the tube was determined as 1.3 kPa in Section 2. The flow rate was set to 300 ml/min, and the pressure was measured using a Pirani gauge (GP-2001G, Ulvac). The incident power was set to three conditions of 100, 200, and 300 W, and the spectroscopic measurements of the CO_2 plasma generated under each microwave incident power were performed. The radiation of the plasma was focused on the slit with a width of 100 μm using a synthetic quartz lens. Table 1 shows the conditions of spectroscopic measurement. Blaze wavelength is representative wavelength of grating in the spectrometer (SR-500, Andor Technology). Two gratings with a blaze wavelength of 300 and 500 nm were used in the spectroscopic measurement. In addition, longpass filters with cut-on wavelength of 320 and 400 nm were used for each wavelength region. After the measurement, the sensitivity was calibrated using a 30 W deuterium lamp in the wavelength region of 200 to 400 nm and a 200 W tungsten halogen lamp in the wavelength region of 350 to 800 nm. Three spectra were obtained by measuring

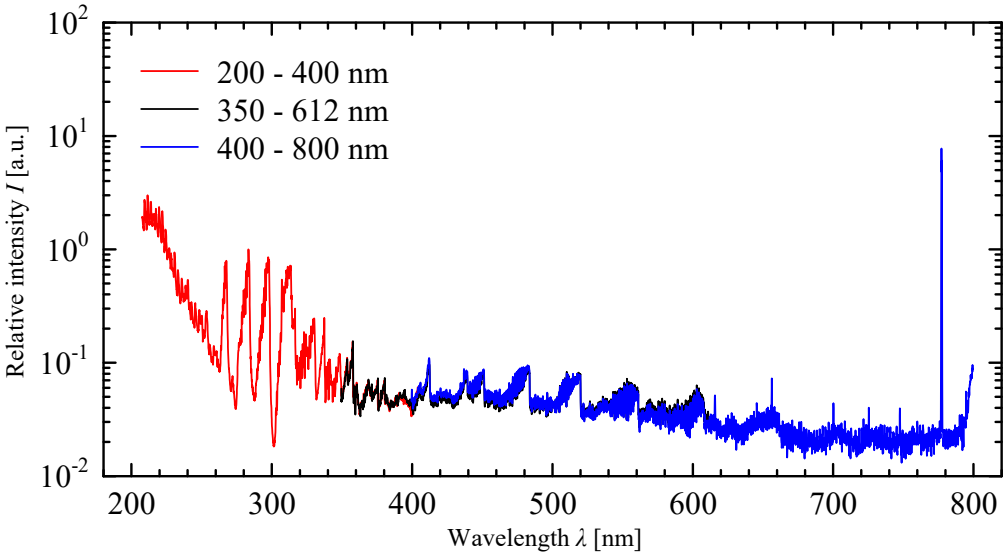

Fig. 3. Comparison of spectra of CO_2 plasma in three wavelength regions (300 W).

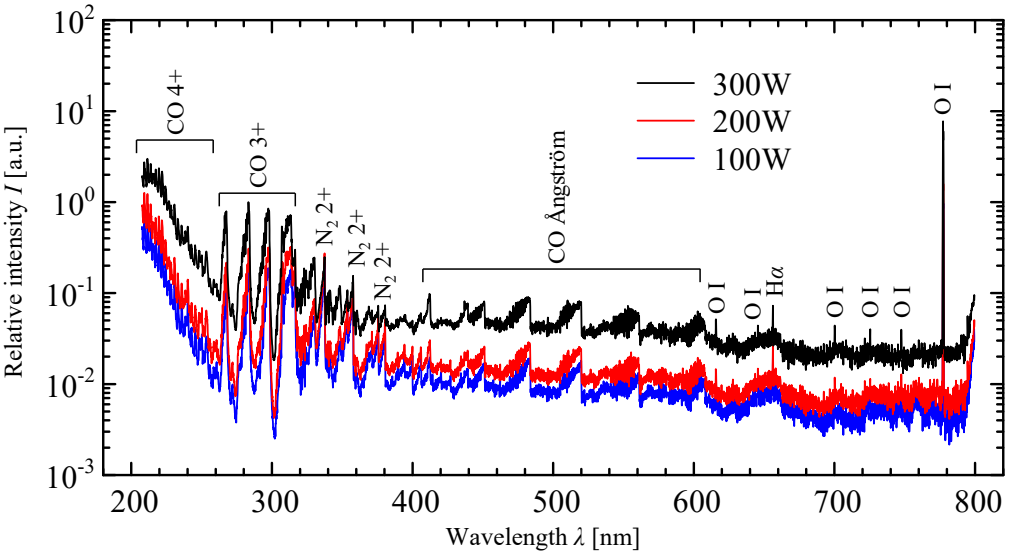

Fig. 4. Comparison of spectra under different conditions of microwave incident powers.

under some conditions of blaze wavelength and filters shown in Table 1, and calibrated using the standard light source corresponding the wavelength region. Figure 3 shows, on a logarithmic scale, the comparison of the spectra in three wavelength regions. Each spectrum was adjusted so that the intensity distribution in the overlapped wavelength region was almost matched, and normalized with the intensity of CO third positive (3+) (0,0) band head. The spectra were combined into one spectrum.

4. Results of Spectroscopic Measurements

Figure 4 shows, on a logarithmic scale, the spectra of CO_2 plasma under the different conditions of microwave incident powers. The spectra are normalized with the intensity of CO 3+ (0,0) band head for 300 W. CO fourth positive (4+) band system, CO 3+ band system, CO Ångström band system and atomic oxygen lines were observed. CO 4+ band system is generated by the transition of the $A^1\Pi$ state to the $X^1\Sigma$ (ground) state. CO 3+ band system is generated by the transition of the $b^3\Sigma$ state to the $a^3\Pi$ state. CO Ångström band system is generated by the transition of the $B^1\Sigma$ state to the $A^1\Pi$ state. O I in the figure means neutral or uncharged oxygen atom. These band systems are typical spectra of microwave-discharged CO_2 plasma.[10] Meanwhile C_2 swan bands and O I are predominant in the CO_2 plasma of arc-heated wind tunnels.[4] This suggests that dissociation of CO into C and O does not occur because microwave-discharged plasma has relatively low enthalpy. It is also found from the figure that the radiation intensity increased when the microwave incident power increased. Electrons in the quartz tube are accelerated by the electric field in the cavity and collide with CO_2 molecules. Then CO_2 molecules dissociate into CO molecules and oxygen atoms. In addition, background continuous radiation overlapped. This emission is due to the chemiluminescence accompanying the recombination of CO and O.[11] As the microwave incident power increases, firstly the electric field in the cavity becomes stronger. Secondly, electrons are accelerated more. Thirdly, particle-electron collisions increase. Finally, dissociation of CO_2 and recombination of CO and O

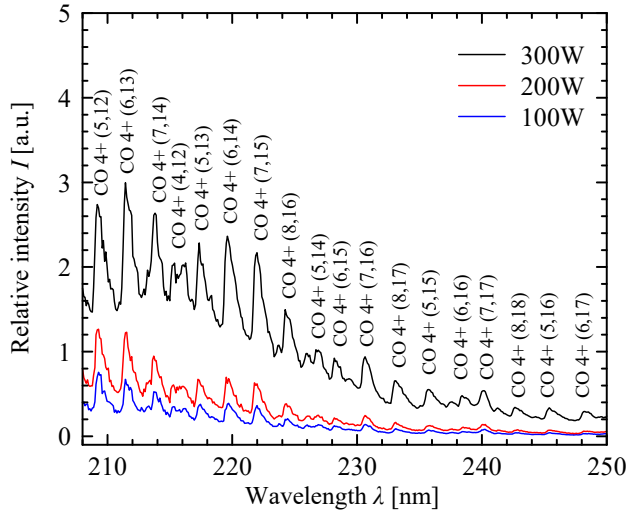

(a) CO 4+ band system (208 - 250 nm).

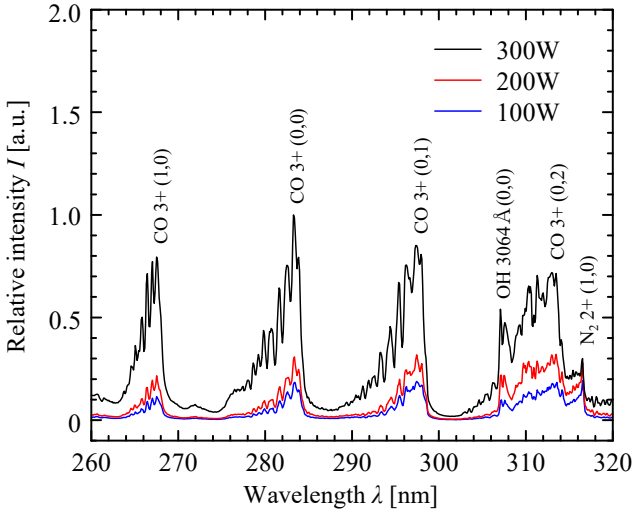

(b) CO 3+ band system (260 - 320 nm).

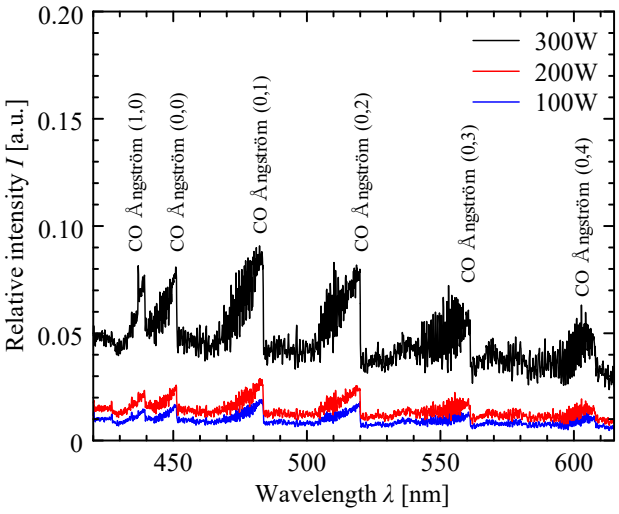

(c) CO Ångström band system (420 - 615 nm).

Fig. 5. Characteristic spectra of CO_2 plasma.

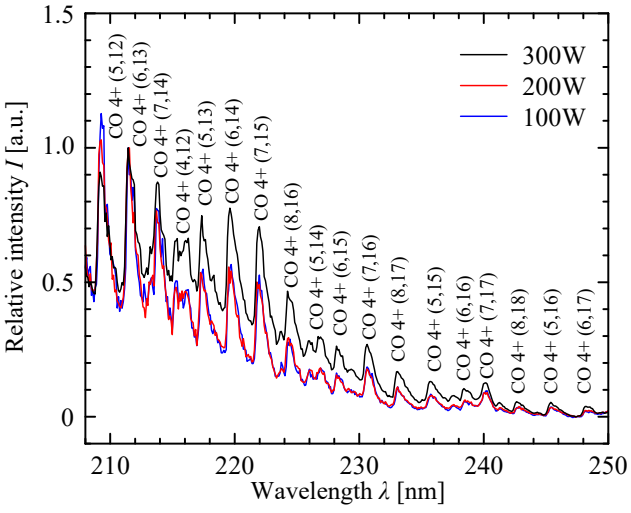

(a) CO 4+ band system (208 - 250 nm).

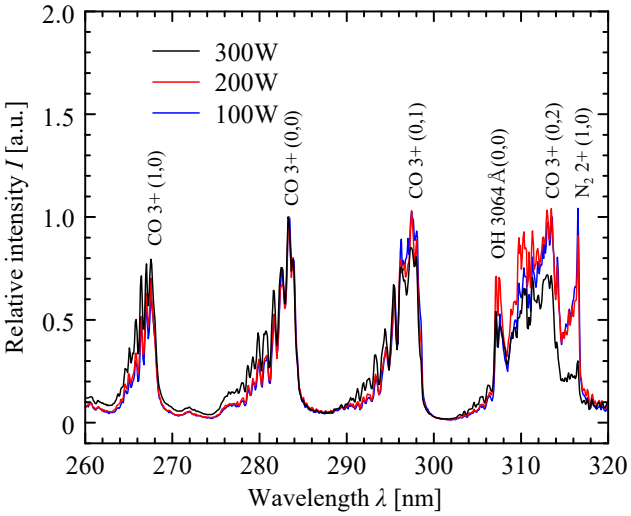

(b) CO 3+ band system (260 - 320 nm).

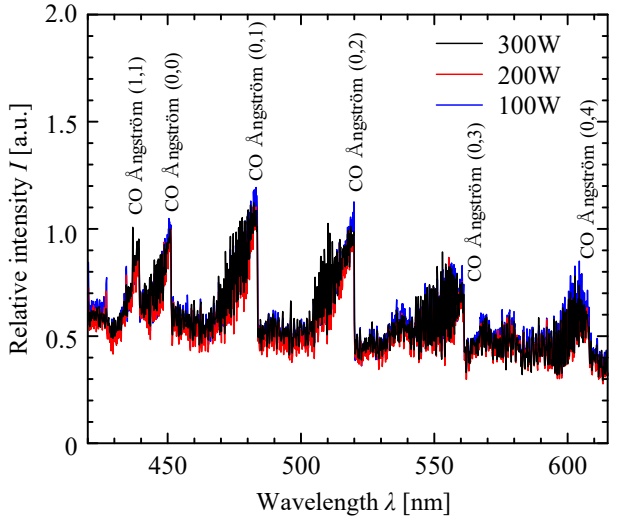

(c) CO Ångström band system (420 - 615 nm).

Fig. 6. Comparison of shape of spectra under different conditions of microwave incident power.

increase. As a result, the radiation intensity increases. The chemical species unrelated to CO_2, such as N_2 second positive (2+) band system and atomic hydrogen line (Hα) were also observed. It is considered that they were generated from impurities.

Figures 5 (a), (b), and (c) show, on a linear scale, characteristic spectra of the CO_2 plasma. The identified molecular band system's names are shown in the figures.[12] The numbers (v', v'') behind the band system's names represent the vibrational quantum numbers, where the upper level is v' and the lower level is v''. Figure 5 (a) shows that CO 4+ band system is predominant in the wavelength region of 208 to 250 nm. The intensity of CO 4+ band system tends to be higher in the shorter wavelength region because the center of CO 4+ band system is in the vacuum ultra violet region shorter than 200 nm. Figure 5 (b) shows that CO 3+ band system is predominant in the wavelength region of 260 to 320 nm. OH 3064Å (0,0) band and N_2 2+ (1,0) band are also observed in the figure. They are derived from impurities. Figure 5 (c) shows that CO Ångström band system is predominant in the wavelength region of 420 to 615 nm.

Figures 6 (a), (b), and (c) show comparison of the shape of the spectra under the different conditions of microwave incident powers to investigate influence of change of the incident power. Figure 6 (a) shows the spectra normalized with the relative intensity of CO 4+ (6,13) band heads under each incident power condition. The spectra for 100 and 200 W are similar in shape, however one for 300 W is different from them. It is also found that the intensity of CO 4+ bands with higher vibrational quantum number of upper level is higher as the incident power increases from 200 to 300 W. It is considered that the vibrational temperature of CO 4+ band system increases. Figure 6 (b) shows the spectra normalized with the relative intensity of CO 3+ (0,0) band heads under each incident power condition. The spectra for 100 and 200 W are similar in shape. The shape of the spectrum does not greatly change as the incident power increases from 200 to 300 W. The intensity distribution of CO 3+ (0,0) band increases as the incident power increases from 200 to 300 W. This suggests that the rotational temperature of CO 3+ band system increases. The intensity of N_2 2+ (1,0) band decreases greatly from 200 to 300 W because the radiation of the CO 3+ bands relatively increase in comparison with N_2 2+ (1,0) band. Figure 6 (c) shows the spectra normalized with the relative intensity of CO Ångström (0,0) band head under each incident power condition. CO Ångström band system does not also change greatly with the increase in microwave incident power, however the intensity distribution of CO Ångström bands increases a little in shorter wavelength region on each band head as the incident power increases from 200 to 300 W. This suggests that the rotational temperature of CO Ångström band system increases. Thus, CO 4 + band system shows a change in vibrational temperature, and CO 3+ and CO Ångström band system show a change in rotational temperature. The obtained spectra need to be compared with the theoretical spectra to estimate rotational and vibrational temperature of CO molecular band system in the future.

5. Estimation of Electronic Excitation Temperature

Electronic excitation temperature was estimated by the Boltzmann plot method,[13] for observed atomic oxygen lines. The Boltzmann plot method is a method to obtain the electronic excitation temperature from the relative ratio of atomic line intensities of the same atom. Equation (1) is used in the Boltzmann plot method.

$$\ln\left(\frac{I_{21}\,\lambda_{21}}{A_{21}g_2}\right) = -\frac{E_2}{\mathrm{k}T_{\mathrm{ex}}} + \ln \mathrm{C}\,, \tag{1}$$

where I_{21} is the intensity of atomic line, λ_{21} is wavelength of atomic line, A_{21} is transition probability, g is multiplicity, E is energy of level, k is Boltzmann constant, T_{ex} is electronic excitation temperature and C is constant common to the spectra of the same temperature and atom. Also, the subscripts indicate that 2 is an upper level, 1 is a lower level, and 21 is a transition from the upper level to the lower level. I_{21} is the value obtained by the measurement, and the other variables are from the known transition data.[14] Table 2 shows the transition data for each atomic line. When the vertical axis is the left side of Eq. (1) and the horizontal axis is E_2, electronic excitation temperature is obtained from the slope $-1/\mathrm{k}T_{\mathrm{ex}}$. Figure 7 shows five atomic oxygen lines for the estimation in the wavelength region of 600 to 800 nm. In this wavelength region, it is considered that atomic oxygen lines overlapped on the continuous radiation. Considering this continuous radiation, the intensity of atomic line I_{21} was determined as the value that relative intensity of peak of atomic line minus relative intensity of continuous radiation. The intensity of continuous radiation was assumed as the minimum intensity within

Table 2. Atomic transition data of oxygen.[14]

Wavelength λ_{21} [nm]	Upper level energy E_2 [cm^{-1}]	Multiplicity g_2 [-]	Transition probability A_{21} [10^8 s^{-1}]	Uncertainties [%]
615.73	102865.56	25	0.0762	< 10
645.50	102116.698	5	0.0826	< 10
700.21	102908.42	15	0.0353	< 10
725.44	102411.995	3	0.0671	< 10
777.34	86629.09	15	0.369	< 3

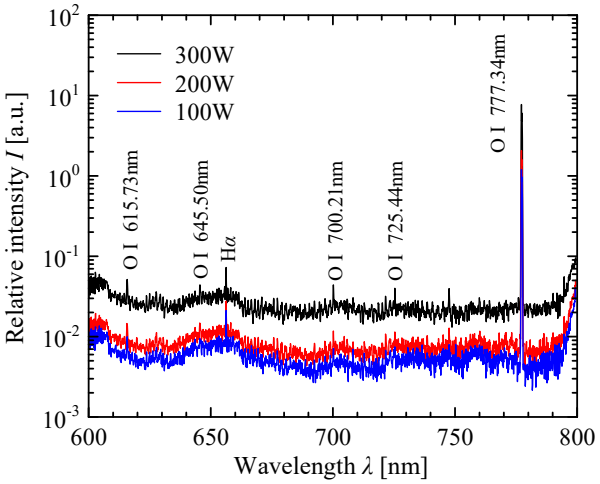

Fig. 7. Atomic oxygen lines.

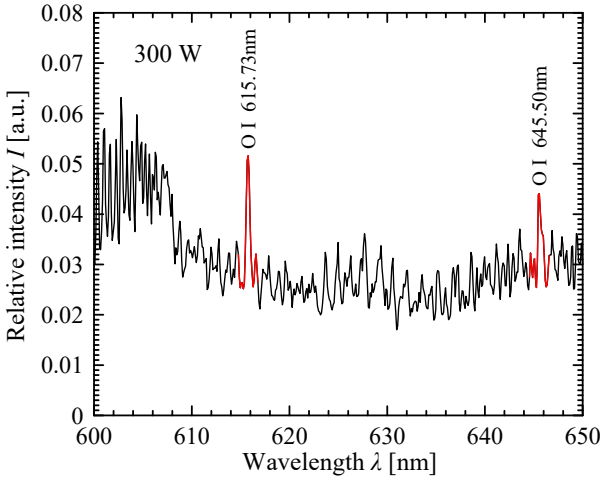

Fig. 8. Range of ±1 nm for atomic oxygen lines.

± 1 nm of the peak of atomic line. In Fig. 8, the red lines show ranges of ±1 nm of atomic oxygen lines with 615.73 and 645.50 nm. The intensity of continuous radiation was assumed as the minimum intensity of red line, and the intensity of atomic line was determined as the value that the relative intensity of peak of atomic line minus the minimum intensity.

Figure 9 shows the Boltzmann plot of the plasma for 300 W of the microwave incident power. The each plot is datum of a oxygen line, and the each error bar is from uncertainty of transition probability. Approximate line was obtained by least square method for the plots, and shown as a black solid line. The maximum and minimum slopes were obtained for the error bars, and shown as red and blue dot lines. The electronic excitation temperature and error range of temperature were estimated from the slopes of the lines. The temperatures of the plasmas for 100 and 200 W were estimated in the same manner. Figure 10 shows estimated electronic excitation temperature. The plots mean temperatures estimated from the slope of the approximate line. The error bars mean temperatures estimated from the maximum slope and minimum slope in Fig. 9. The estimated temperature is about 6,300 K under any microwave incident power conditions of 100, 200, and 300 W. However, the estimated temperatures have wide error ranges with 4,700-9,300 K. Therefore, it is difficult to discuss the order of temperature range with the microwave incident power. It is considered that the increase in energy given by the microwave is hardly consumed for the excitation of oxygen, and it is mainly consumed for the increase in the temperatures of CO 4+ band system, CO 3+ band system, and continuous radiation. In the future, spectroscopic measurements in near-infrared region will be performed to investigate radiative characteristics of the CO_2 plasma in near-infrared region and to obtain other atomic oxygen lines. In addition, argon gas will be added to the CO_2 plasma and the electronic excitation temperature will be estimated from the atomic argon lines to check the validity of the temperature.

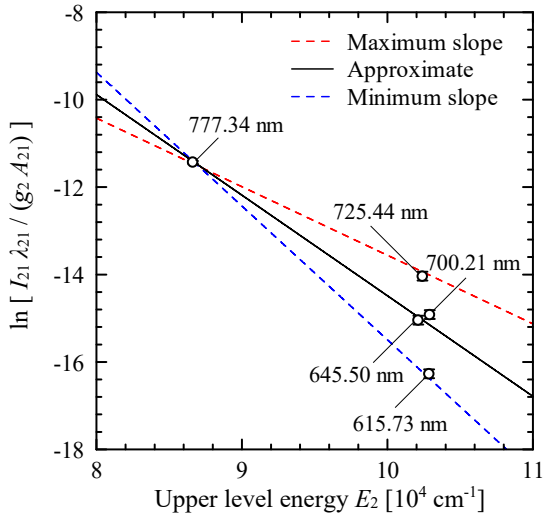

Fig. 9. Boltzmann plot for atomic oxygen lines (300 W).

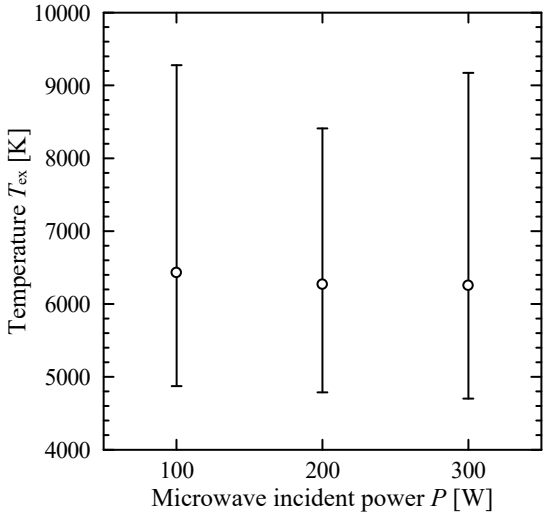

Fig. 10. Estimated electronic excitation temperature.

6. Conclusion

The microwave-discharged CO_2 plasma was generated under the pressure condition predicted during Mars entry and

measured spectroscopically. The differences of the radiative characteristics with microwave incident power were investigated, and electronic excitation temperatures of the plasmas were estimated by the Boltzmann plot method for atomic oxygen lines. The main conclusions are shown as follows.

(1) The radiation intensity increases with the increase in microwave incident power.
(2) CO molecular band systems and atomic oxygen lines are predominant in the radiation of microwave-discharged CO_2 plasma because CO_2 molecules dissociate into CO molecules and oxygen atoms.
(3) The radiative characteristics of CO_2 plasma for 100 and 200 W are similar in shape, however one for 300 W is different from them.
(4) The electronic excitation temperatures for atomic oxygen lines were estimated to be about 6,300 K, however there was at least an error range of 4,700-9,300 K.
(5) Estimated electronic excitation temperature was almost the same if microwave incident power changed.

References

1) Fujii, A. and Arafune, Y.: *Science of Mars*, Seibundo Shinkosha Publishing, Tokyo, 2018, pp. 106-109, 118-121 (in Japanese).
2) Gnoffo, P. A., Weilmuenster, K. J., Braun, R. D., and Cruz, C. I.: Effects of Sonic Line Transition on Aerothermodynamics of the Mars Pathfinder Probe, AIAA Paper 95-1825, 1995.
3) Brandis, A. M., Saunders, D. A., Johnston, C. O., Cruden, B. A., and White, T. R.: Radiative Heating on the After-Body of Martian Entry Vehicles, 45th AIAA Thermophysics Conference, Dallas, U. S. A., ARC-E-DAA-TN23559, 2015.
4) Yamada, G., Otsuta, S., Matsuno, T., and Kawazoe, H.: Temperature Measurements of CO_2 and CO_2-N_2 Plasma Flows around a Bulent Body in an Arc-Heated Wind Tunnel, *Trans. JSASS Aerospace Tech. Japan*, **11** (2013), pp. 87-91.
5) Rond, C., Boubert, P., Félio, J.-M., and Chikhaoui, A.: Nonequilibrium radiation behind a strong shock wave in CO_2-N_2, *Chem. Phys.*, **340** (2007), pp. 93-104.
6) Babou, Y., Rivière, P., Perrin, M. Y., and Soufiani, A.: Spectroscopic Data for the Prediction of Radiative Transfer in CO_2- N_2 Plasmas, *J. Quant. Spectrosc. Radiat. Transf.*, **110** (2009), pp. 89-108.
7) Mahaffy, P. R., Webster, C. R., Atreya, S. K., Franz, H., Wong, M., Conrad, P. G., et al.: Abundance and Isotopic Composition of Gases in the Martian Atmosphere from the Curiosity Rover, *Science*, **341** (2013), pp. 263-266.
8) Matsuo, K.: *Compressible Fluid Dynamics*, Rikogakusha Publishing, Tokyo, 1994, p. 107 (in Japanese).
9) Shibusawa, K and Funatsu, M.: Radiative Characteristics of N_2 First Positive Band in Visible and Near-infrared Regions for Microwave-discharged Nitrogen Plasma, *Trans. Jpn. Soc. Aeronaut. Space Sci.*, **62** (2019), pp. 86-92.
10) Leins, M., Gaiser, S., Kopecki, J., Bongers, W. A., Goede, A., Graswinckel, M. F., et al.: Dissociation of CO_2 by Means of a Microwave Plasma Process for Solar Fuels Production, Proceedings of 22nd International Symposium on Plasma Chemistry, Antwerp, Belgium, P-II-8-18, 2015.
11) Rond, C., Bultel, A., Boubert, P., and Chéron, B. G.: Spectroscopic Measurements of Nonequilibrium CO_2 Plasma in RF Torch, *Chem. Phys.*, **354** (2008), pp. 16-26.
12) Pearse, R. W. B. and Gaydon, A. G.: *The Identification of Molecular Spectra*, Chapman & Hall, London, 1976, pp. 108-110, 219.
13) Yamamoto, M. and Murayama, S.: *Spectroscopic Measurement of Plasma*, Gakkai Shuppan Center Publishing, Tokyo, 1995, pp. 117-119 (in Japanese).
14) Wiese, W. L., Fuhr, J. R., and Deters, T. M.: Atomic Transition Probabilities of Carbon, Nitrogen, and Oxygen, *J. Phys. Chem. Ref. Data*, Monograph No. 7 (1996), pp. 335-364.